0.0.1 Electron-Cloud Effect

M. A.Furman, LBNL

Background The electron-cloud (or photo-electron) effect (ECE) was first identified at the Photon Factory (PF) at KEK [1] as a fast transverse coupled-bunch instability that arose only when the machine was operated with a positron beam. Unlike the ion-induced instability, which was observed when the PF was operated with an electron beam, the positron beam instability persisted even with a substantial gap in the bunch train. The coupled-bunch mode spectrum for the positron beam was qualitatively different from that for an electron beam under otherwise similar conditions. The phenomenon disappeared when the bunch spacing was sufficiently large, and it could not be attributed to known machine impedances. The amplitude of the unstable motion reached saturation and was accompanied by the excitation of vertical coupled-bunch oscillations, and possibly of vertical emittance growth.

Experimental analysis [1], simulations [2] and analytical work [3] showed that the cause of the instability is an electron cloud (EC) that developed inside the vacuum chamber. The ECE was later studied in dedicated experiments at BEPC and the APS [4,5]. It has led to serious performance limitations at PEP-II and KEKB [6,7]. A related coupled-bunch instability has been observed at CESR [8].

The ECE is related to beam-induced multipacting (BIM), first observed at the ISR [9] when operated with bunched beams. Closely related to BIM is trailing-edge multipacting observed at the PSR [10,11], where electron detectors register a large signal during the passage of the tail of the bunch even for stable beams. ECEs for present-day hadron machines (see below) are related to the e-p instabilities for bunched and unbunched beams first seen at BINP in the mid-60s [12,13].

Phenomenology In positron or electron rings, the EC is initiated when the synchrotron radiation (SR) emitted by the beam leads to photoelectrons upon striking the vacuum chamber. In proton rings, the EC is typically initiated by ionization of residual gas or from electron generation when stray beam particles strike the chamber. The LHC will be the first proton storage ring in which the beam will emit copious SR (critical energy ~ 44 eV), leading to substantial photoemission, hence the mechanism for the formation of the EC will be analogous to present-day positron rings [14].

The above-mentioned primary mechanisms are typically insufficient to lead to significant ECEs. However, these primary electrons are kicked by successive bunches, striking the walls of the vacuum chamber with a broad energy spectrum and leading to secondary electron emission (SEE). This can lead to a large amplification factor (typically a few orders of magnitude) of the primary electron density and to strong time fluctuations in the electron distribution [14–16]. This compounding effect of SEE is usually the main determinant of the average strength of the ECEs, and is particularly strong in positively-charged bunched beams. It is strongest when the BIM resonant condition is satisfied [9].

The ECE combines many parameters of a storage ring such as bunch current, bunch spacing, vacuum chamber geometry, vacuum pressure, and properties of the chamber surface material such as the photon reflectivity R_γ, effective photoelectric yield Y_{eff}, and the secondary electron yield (SEY) function $\delta(E)$ (E =electron-wall impact energy) [17]. A convenient phenomenological parameter is the effective SEY, δ_{eff}, defined to be the average of $\delta(E)$ over all electron-wall collisions during a relevant time window. If $\delta_{\text{eff}} > 1$, the EC grows exponentially following injection of the beam into an empty chamber, with a typical risetime of tens of bunch passages, and is sustained as long as there is beam in the machine. The exponential growth stops when space-charge forces of the electrons suppress further electron emission, and the average electron density reaches a saturation value comparable to the beam neutralization level. If there is a gap in the beam, or if the beam is extracted, the cloud dissipates with a falltime that is controlled by the low-energy value of $\delta(E)$ [18].

Dedicated electron detectors have been designed and used to study the intensity and spectrum of the electrons striking the vacuum chamber [19–22].

Consequences One consequence of the EC is a strong increase in the vacuum pressure as

a function of bunch current. The pressure rise exhibits a threshold behavior, and is sensitive to the bunch fill pattern at fixed total current [6, 7, 21, 24, 25].

The EC can lead to diagnostic problems owing to an effective shielding of the BPMs [26], and to a bunch-to-bunch tune shift that grows towards the tail of the bunch train [27–29]. Single-bunch incoherent effects such as emittance growth have been studied and observed [6, 30–33], or particle losses [11].

In 1996-97, calculations showed that the LHC will be subject to an ECE [34–36]. The main concern here is the power deposited by the electrons rattling around the chamber, which must be dissipated by the cryogenic system if the LHC is to work as specified. Since the cryogenic system was designed before the discovery of the ECE, substantial effort has been devoted at since 1997 to better estimate the power deposition, to identify the conditions under which the cooling capacity may be exceeded, and to devise mitigation mechanisms if necessary [14, 15, 17, 37–43] As part of this effort, the ECE has been studied at the SPS and the PS [21, 26, 44–46] when operated with LHC-style beams.

The ECE has been observed at RHIC where it leads to fast vacuum pressure rise that limits the performance at high beam current [25]. A high-current instability that has been observed for many years at the PSR is also an ECE [11]. The phenomenon has been studied in intense, long-pulse, heavy-ion fusion drivers [22], and at the J-PARC proton rings [47]. A sample simulation result for the EC density is given in Fig. 1.

Mitigating mechanisms A low value of Y_{eff} is favorable, as the EC density is a monotonically increasing function of Y_{eff}. At the LHC small transverse grooves will be engraved on the vacuum chamber, effectively resulting in normal photon incidence thus leading to a reducion of Y_{eff} by a factor of 2–4, and R_γ by a factor ~ 10. This mechanism has been successfully demonstrated [48, 49].

Y_{eff} can also be reduced by an antechamber on the outboard side of the vacuum chamber. At PEP-II [23], the antechamber allows for $\sim 99\%$ of the photons to escape out of the vacuum chamber. The remaining 1% of the photons, however, are radiated at wide angle
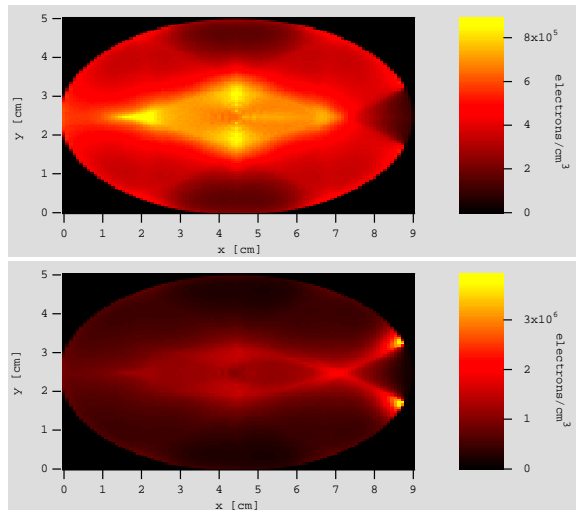
Figure 1: Simulated time-averaged electron density in a field-free region in the arcs of the PEP-II positron ring. Top: $R_\gamma \simeq 1$. Bottom: $R_\gamma \simeq 0$. The beam (not shown) travels perpendicularly to the page through the center of the chamber. The low-density region to the right of the chamber is due to the electrons escaping through the antechamber slot [23].

and low energy, and generate photoelectrons more efficiently [50] than the high-energy photons that escape, hence the quantitative advantage of an antechamber *vis à vis* the ECE is not a simple linear function of the number of photons it allows to escape from the chamber.

If SEE is significant, achieving a low value of δ_{eff} is essential, as SEE is typically a much more significant effect than photoemission. Although pure Al has a low peak value of δ, $\delta_{max} \lesssim 1$, its surface is normally covered with a layer of Al_2O_3 with $\delta_{max} \sim 2.5 - 3$, among the highest of all practical metals. For this reason, the Al chambers in the arcs of the PEP-II positron ring have been coated with TiN [51]. This coating, once properly conditioned, has $\delta_{max} \sim 1.1$. TiN coatings will also be used in the SNS [52]. Copper and stainless steel have $\delta_{max} \sim 1.3 - 1.5$ when adequately conditioned. Reducing δ_{max}, however, is not enough: the low-energy ($E \lesssim 10$ eV) value of $\delta(E)$, and certain details of the emission energy spectrum [16, 53–56], can play a significant effect on the survival of the EC during a beam gap and hence on the average EC density. Other coatings, especially TiZrV, is or

will be used in the warm regions of RHIC and the LHC [57, 58], and probably in the ILC damping rings [59]. Longitudinal grooves (along the beam direction) of pitch and depth of a few mm etched on the vacuum chamber walls show promise as effective SEY suppressors in lab tests [60, 61].

The ECE is a self-conditioning effect in the sense that $\delta_{\max}$ gradually decreases owing to the electron bombardment during normal machine operation [11, 21]. The important practical question is how long it takes for $\delta_{\max}$ to fall below a value where the EC is no longer an operational limitation.

Active mechanisms have been used such as raising the vertical chromaticity above its nominal value, or using octupolar fields [62, 63]. Solenoidal windings have been wrapped around most of the circumference of the positron rings of PEP-II and KEKB [64, 65]. A relatively low field ($B = 20 - 30$ G) is sufficient to trap the electrons near the walls of the vacuum chamber, thereby minimizing their effect on the beam. These solenoids have proven essential for the B factories to reach their present-day performance. Elaborate bunch fill patterns have been used at PEP-II [66]. The many gaps in these patterns have the effect of promoting the dissipation of the EC. At the PSR it has been found that increasing the momentum spread of the beam increases the current instability threshold [11]. A clearing electrode with a voltage ~ 100 V has been proposed for the LHC arcs [67].

Besides the usual accelerator conference proceedings, the following Internet sites contain a large number of ECE-related publications:

http://icfa-ecloud04.web.cern.ch/icfa-ecloud04/

http://www.gsi.de/search/events/conferences/ICFA-HB2004/index_e.html

http://www.c-ad.bnl.gov/icfa/

http://wwwslap.cern.ch/collective/ecloud02

http://conference.kek.jp/two-stream/

http://www.aps.anl.gov/conferences/icfa/two-stream.html

http://www-acc.kek.jp/WWW-ACC-exp/Conferences/MBI97-N/MBI97.html

http://www.aps.anl.gov/asd/physics/ecloud/ecloud.html

References

[1] M. Izawa *et al.*, PRL **74**, 5044 (1995).

[2] K. Ohmi, PRL **75**, 1526 (1995).

[3] S. Heifets, CEIBA95.

[4] Z. Y. Guo *et al.*, PAC97.

[5] K. C. Harkay, PAC99.

[6] A. Kulikov *et al.*, PAC01.

[7] H. Fukuma *et al.*, EPAC00.

[8] J. T. Rogers, PAC97.

[9] O. Gröbner, HEACC77.

[10] V. Danilov *et al.*, AIP Conf. Proc. No. 496.

[11] R. J. Macek *et al.*, ECLOUD04.

[12] V. Dudnikov, Pressure Rise Mini Wkshp., BNL, 2003.

[13] V. Dudnikov, PAC01.

[14] G. Rumolo *et al.*, PRST-AB **4**, 012801 (2001). Erratum: **4**, 029901 (2001).

[15] M. A. Furman, LHC-PR-180.

[16] M. A. Furman *et al.*, LBNL-59062.

[17] F. Zimmermann, ECLOUD04.

[18] M. A. Furman, PAC03.

[19] R. A. Rosenberg *et al.*, NIMPR **A453**, 507 (2000).

[20] R. Macek *et al.*, PAC03.

[21] J. M. Jiménez *et al.*, LHC-PR-632.

[22] A. W.Molvik *et al.*, PAC05.

[23] M. A. Furman *et al.*, MBI97.

[24] G. Arduini *et al.*, ECLOUD04.

[25] W. Fischer *et al.*, ECLOUD04.

[26] R. Cappi *et al.*, PAC01.

[27] K. Cornelis, ECLOUD02.

[28] T. Ieiri *et al.*, Two-Stream Instabil. Wkshp., KEK, 2001.

[29] K. Ohmi, Two-Stream Instabil. Wkshp., KEK, 2001.

[30] E. Perevedentsev, Two-Stream Instabil. Wkshp., KEK, 2001.

[31] M. A. Furman *et al.*, PAC99.

[32] K. Ohmi *et al.*, PRL **85**, 3821 (2000).

[33] H. Fukuma, Two-Stream Instabil. Wkshp., KEK, 2001.

[34] O. Gröbner, Vacuum **47**, 591 (1996).

[35] O. Gröbner, PAC97.

[36] F. Zimmermann, LHC-PR-95.

[37] G. V. Stupakov, LHC-PR-141.

[38] O. S. Brüning, LHC-PR-158.

[39] EC in the LHC, http://ab-abp-rlc.web.cern.ch/ab%2Dabp%2Drlc%2Decloud/

[40] V. Baglin, http://at-div-vac.web.cern.ch/at-div-vac/VACPAGES/ps/Phys&tech/Phys/Ecloud/SEY/SEY_ paper.html

[41] F. Zimmermann, ECLOUD02.

[42] F. Zimmermann, ICFA Beam Dynamics Newsletter **31**.

[43] F. Zimmermann *et al.*, ICFA Beam Dynamics Newsletter **32**.

[44] G. Arduini *et al.*, PAC01.

[45] M. Giovannozzi *et al.*, PRST-AB **6**, 010101 (2003).

[46] R. Cappi *et al.*, PRST-AB **5**, 094401 (2002).

[47] T. Toyama, ECLOUD04.

[48] O. Gröbner, Two-Stream Instabil. Wkshp., S. Fe, 2000.

[49] V. Baglin *et al.*, EPAC98.

[50] O. Gröbner *et al.*, J. Vac. Sci. Technol. **A7**, 223 (1989).

[51] K. Kennedy *et al.*, PAC97.

[52] P. He *et al.*, PAC01.

[53] V. Baglin *et al.*, LHC-PR-472.

[54] N. Hilleret, Two-Stream Instabil. Wkshp, KEK, 2001.

[55] R. Cimino *et al.*, PRL **93**, 014801 (2004).

[56] R. E. Kirby *et al.*, NIMPR **A469**, 1 (2001).

[57] H. C. Hseuh *et al.*, PAC05.

[58] LHC Design Report, CERN-2004-003, **1**, p. 346

[59] M. Pivi *et al.*, PAC05.

[60] A. A. Krasnov, Vacuum **73**, 195 (2004).

[61] G. Stupakov *et al.*, ECLOUD04.

[62] Z. Y. Guo *et al.*, MBI97.

[63] H. Fukuma, Two-Stream Instabil. Wkshp, S. Fe, 2000.

[64] A. Kulikov *et al.*, ECLOUD04.

[65] H. Fukuma, ECLOUD04.

[66] F.-J. Decker *et al.*, PAC01.

[67] P. McIntyre *et al.*, PAC05.